



Spherical Phaseless Probe-Corrected Near-Field Measurements of the DTU-ESA VAST12 Reflector Antenna

Fernandez Alvarez, Javier; Bjørstorp, Jeppe Majlund; Breinbjerg, Olav

Published in:

Proceedings of the 40th Annual Meeting and Symposium of the Antenna Measurement Techniques Association

Publication date:

2018

Document Version

Peer reviewed version

[Link back to DTU Orbit](#)

Citation (APA):

Fernandez Alvarez, J., Bjørstorp, J. M., & Breinbjerg, O. (2018). Spherical Phaseless Probe-Corrected Near-Field Measurements of the DTU-ESA VAST12 Reflector Antenna. In *Proceedings of the 40th Annual Meeting and Symposium of the Antenna Measurement Techniques Association* (pp. 216-221). IEEE.

General rights

Copyright and moral rights for the publications made accessible in the public portal are retained by the authors and/or other copyright owners and it is a condition of accessing publications that users recognise and abide by the legal requirements associated with these rights.

- Users may download and print one copy of any publication from the public portal for the purpose of private study or research.
- You may not further distribute the material or use it for any profit-making activity or commercial gain
- You may freely distribute the URL identifying the publication in the public portal

If you believe that this document breaches copyright please contact us providing details, and we will remove access to the work immediately and investigate your claim.

Spherical Phaseless Probe-Corrected Near-Field Measurements of the DTU-ESA VAST12 Reflector Antenna

Javier Fernández Álvarez, Jeppe M. Bjørstorp and Olav Breinbjerg
Department of Electrical Engineering, Technical University of Denmark, DTU
Kgs Lyngby, Denmark
jafealv@elektro.dtu.dk, jmn@elektro.dtu.dk, ob@elektro.dtu.dk

Abstract—An experimental case of spherical probe-corrected phaseless near-field measurements with the two-scans technique is presented, based on magnitude measurements at two surfaces of the VAST12 reflector antenna performed at the DTU-ESA Facility.

Phase retrieval using strictly the directly measured near-field magnitude was unfeasible in this setup, due to the small sphere separation allowed by the probe positioner, which led to incorrect and excessively slow convergence. Phase retrieval with larger separation between spheres has shown remarkable results. For these tests a measured magnitude was used in combination with calculated near-field magnitudes at different (larger and smaller) spheres with larger separations than allowed by the experimental setup. It has been seen that larger separation between measurement spheres improves accuracy of phase retrieval.

A measurement with a backprojected measurement with 3 m sphere separation is of particular interest because it can be potentially replicated in the DTU-ESA Facility assuming such range of movement was allowed, while being accurate down to an error of less than -35dB. Measurements with larger spheres show even better accuracy.

These good results were obtained with the normal spatial sampling rate for complex measurements and with a very simple Hertzian dipole initial guess, and show the superior performance of spherical phaseless measurements with the two-scans technique, compared to a planar setup.

I. INTRODUCTION

Phaseless near-field measurements are a family of techniques which aim to obtain the phase of a signal by means other than direct measurement; typically by performing more measurements of the magnitude of said signal than necessary for a complex measurement, and deploying a mathematical algorithm that uses said magnitude data to obtain the phase of the signal [1]–[7]. Phaseless measurements are a desirable alternative when complex measurement are impractical or unreliable; one case is high-frequency measurements when the fast-changing phase measure is significantly affected by inaccuracies of measurement equipment or probe positioning, cable bending, thermal drift, etc; while the magnitude of the measured signal is not significantly affected by these factors and therefore can be measured more reliably.

The two-scans technique is based on a pair of magnitude measurements at two different distances from the antenna under test (AUT), and relies in the propagation relation between the fields at these two surfaces in order to retrieve a phase. This algorithm requires an initial guess for the phase, with which one of the magnitude measurements is augmented to create a complex field.

While this technique is well documented, most of the available results, both experimental and simulations, concern planar near-field measurements, with the spherical case being comparatively less studied [8]–[10].

In this paper we present a spherical phaseless near-field measurement of the VAST12 (VALidation STandard) antenna based on measurements at different radii, which were performed at the DTU-ESA Spherical Near-Field Antenna Test Facility. This spherical range allows for measurements at different radii by mounting the probe on a translation stage on top of a fixed probe positioner, allowing for a limited range of separation between measurements. The two-scans technique generally benefits from larger separation between measurement surfaces, which usually translates to greater difference between the two sets of measured magnitudes. In order to increase the radius of the measurements beyond what is allowed by the measurement setup, near-fields at different radii are calculated by means of spherical wave expansion (SWE). A comparison between the different measurements is then established, in order to assess the accuracy of the two-scans technique, and to study the influence of sphere separation in the performance of the phase retrieval.

This manuscript is structured as follows: in Section II a description of the measurement setup and the AUT is given, in Section III the two-scans phaseless near-field technique is summarized, in Section IV the phaseless measurements using direct measurements of the AUT magnitude as well as calculated by means of SWE are presented and discussed, in Section V phase retrieval in spherical and planar setups are compared, and Section VI contains the conclusions.

II. MEASUREMENT SETUP AND VAST12 ANTENNA

The DTU-ESA Spherical Near-Field Antenna Test Facility is operated by DTU as an external reference laboratory for the European Space Agency (ESA) for high-accuracy antenna measurements and calibrations. The anechoic chamber measures 15m x 12m x 12m between absorbers. Measurements are done as spherical scanning by rotation, roll-over-azimuth, of the AUT. The probe is situated atop a static probe tower; the distance between AUT and probe origin of coordinates is approximately 6 m. The probe scans the spherical surface on a discrete regular grid in an appropriate number of sample points. The probe tower allows for a displacement of the probe antenna in the z-axis, however the distance allowed is currently of only 50 mm.

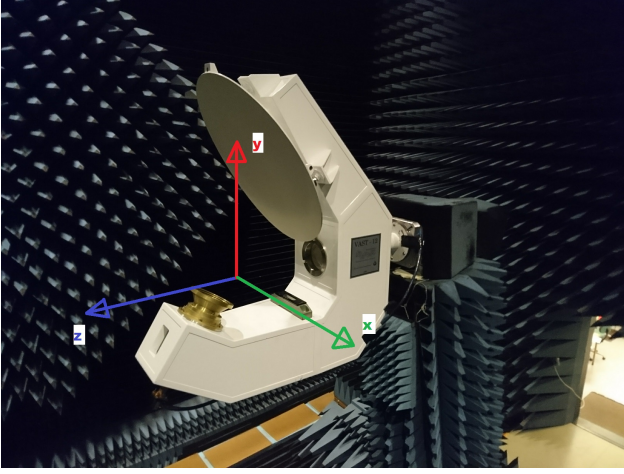


Fig. 1. VAST12 antenna mounted in the DTU-ESA Facility antenna positioner, with superimposed AUT coordinate system.

The RF system consists of a MI-3103 signal source and a MI-1797 receiver. These, together with the data acquisition system, are controlled by an MI-3000 workstation. Processing of the data, including near-field to far-field transformation, is performed using software developed by DTU and TICRA, such as SNIFTD [11][12].

The VAST12 antenna, shown in Fig. 1, was developed at DTU for ESA as a reference antenna, with the goal of having a tool to compare and benchmark different antenna measurement facilities with an antenna that is very thermally and mechanically stable. This means that deformations in the antenna structure due to dilation/contraction due to temperature changes, as well as deformation caused by gravity as the antenna is rotated, are minimum; thus the antenna reliably provides a similar radiation pattern independently of the characteristics on the medium in which it is measured: uncertainty introduced by deformations of the antenna is of 0.01dB [13]-[15].

The AUT consists of an offset, shaped parabolic reflector with different focal points in the two main planes, and a corrugated circular feed horn mounted on a structure of carbon fiber reinforced polymer (CFRP) and foam to achieve the desired mechanical/thermal properties. The shaped reflector provides an elliptical main beam and several challenging characteristics, such as sidelobes and minima of varying levels [14]. In its present configuration it is linearly polarized with orientation of the electric field in the offset plane ($\phi = 90$).

The probe used for the 12 GHz measurements is a standard DTU-ESA Facility dual-ported conical horn with a frequency range of 10.8 to 12.4 GHz. The data was sampled at intervals of 0.5 deg in θ and 1 deg in ϕ .

III. PHASELESS SPHERICAL NEAR-FIELD TECHNIQUE

Let w_1, w_2 be the near-field signals at two different measurement surfaces S_1, S_2 , and $M_1 = |w_1|, M_2 = |w_2|$ the magnitude of said near-field signals. In order to reconstruct the phase of the near-field, the two-scans technique [1] uses the analytic relation between the fields at each measurement sphere given by the transmission formula [16],

$$w(r, \theta, \phi, \chi) = \sum_i T_i C_i(r, \theta, \phi, \chi) R_i \quad (1)$$

where (r, θ, ϕ) are the spherical coordinates of the probe position, and χ the probe orientation angle. The rotation-translation coefficients C_i are known functions and R_i are the probe receiving coefficients, also assumed to be known from a calibration of the probe. The magnitude of w is known from the near-field magnitude measurements. Thus the AUT transmitting coefficients T_i are to be determined; this is done by generating two different configurations of eq. (1) for which an analytic relationship exists between the probe signals. In this case, by changing the measurement distances the rotation-translation coefficients $C_i(r, \theta, \phi, \chi)$ are changed.

A phaseless measurement starts with the magnitude at the first sphere M_1 , combined with an initial guess Φ_0 for the phase in order to generate a *first complex field*, $\tilde{w}_1 = M_1 e^{j\Phi_0}$. As is generally the case, the initial guess phase must be such that the first complex field does not contain discontinuities arising from a 180-deg phase change in points where the measured magnitude is non-zero. Phase retrieval consists of the following steps:

- \tilde{w}_1 is propagated from S_1 to S_2 by means of spherical wave expansion, obtaining a new calculated complex field, $\tilde{w}_2 = |\tilde{w}_2| e^{j\Phi_{w_2}}$.
- $|\tilde{w}_2|$ is compared to the measured magnitude M_2 by means of a certain near-field error metric.
- $|\tilde{w}_2|$ is discarded and substituted with M_2 , resulting in complex field $\tilde{w}_2' = M_2 e^{j\Phi_{w_2}}$.
- \tilde{w}_2' is then propagated to S_1 .
- The iterative process of propagation and magnitude substitution is continued after a certain stopping condition is met.

The stopping condition is typically when the near-field error metric becomes smaller than a certain threshold (ideally indicating the correct convergence of the algorithm to within the desired accuracy), or when a maximum number of iterations is reached.

The two-scans technique is a non-linear, ill-posed technique. Optimally, the phase of the initial guess will over successive iterations converge into the global minimum of the solution space of the phase, which corresponds to the actual phase of the signals measured at the scan planes. In practice this is not always true, and the two-scans technique is sensitive to parameters like separation between measurement surfaces, choice of initial guess, or dynamic range of the measurement. These factors may cause the phase to become trapped in a local minimum of the solution space, resulting in convergence to a false phase for the AUT.

From eq. (1) it is also understood that the probe receiving coefficients R_i are necessary to solve the transmission formula for T_i ; this is done by the SNIFTD software, which makes use of the probe receiving coefficients to calculate the T_i of the AUT and the sphere-to-sphere transformation at each step of the iterative process. Thus, probe correction is an integral part of the phase retrieval itself, applied at each step of the iterative phase retrieval.

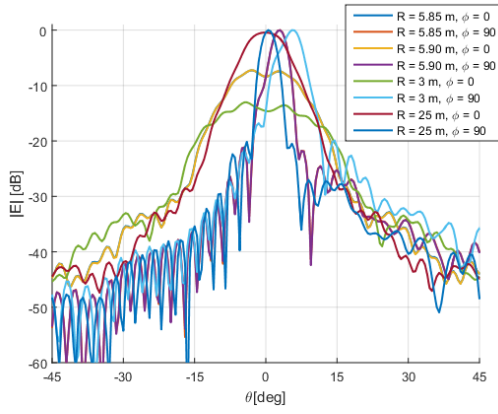


Fig. 2. Near-field magnitude $\phi = 0, 90$ cuts of experimental measurements with radius $r = 5.835$ m, $r = 5.903$ m, and calculated near-fields at spheres of $r = 3$ m and $r = 25$ m. It is noted that measured curves are almost totally on top of each other due to the small (50 mm) separation.

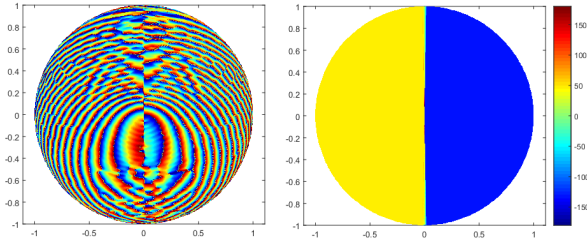


Fig. 3. Forward hemisphere phase u-v plots of complex full-sphere measured near-field signal ϕ component at nominal distance of 5.8 m (left) and ϕ component phase of Hertzian dipole (right).

IV. RESULTS AND DISCUSSION

The phaseless measurements studied in this section are based on two complex spherical measurements of the AUT: Measurement 1 with radius of 5853 mm (234λ) and Measurement 2 with radius of 5903 mm (236λ); thus separation is of 50 mm (2λ) which is the maximum allowed by the probe positioner. It is seen in Fig. 2 that the near-field magnitudes of these two measurements are very similar.

From Measurement 1 a probe-corrected reference far-field measurement is obtained by means of the usual near-field to far-field transformation. This reference pattern will be used to compare all subsequent phaseless measurements.

The initial guess for all phaseless measurements in this paper is the phase of a y-oriented Hertzian dipole located at the AUT origin of coordinates. This dipole is conveniently oriented according to the guidelines in Section III to avoid a discontinuous field. In Fig. 3 it is seen that the phase of the Hertzian dipole jumps in the same points as the real phase; these are points where magnitude is null.

A. Phase retrieval for measurement spheres with small separation

In the first phaseless measurement only the purely measured magnitudes of Measurements 1 and 2 are considered. Given the very small range of horizontal displacement allowed by the probe positioner, separation between spheres is only 2λ , or

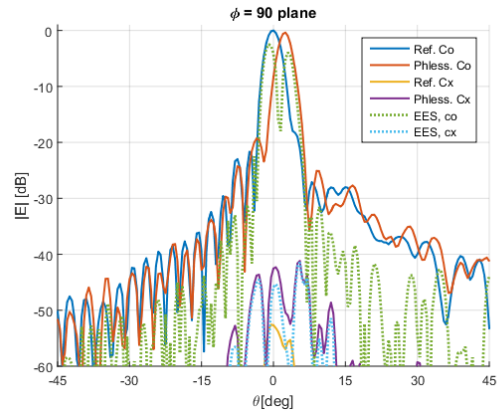


Fig. 4. E-plane ($\phi = 90$) radiation pattern of phaseless measurement with small sphere separation compared to reference measured radiation pattern.

$< 1\%$ of the probe-AUT separation. The phase retrieval uses a fixed number of 50,000 iterations.

A point-by-point far-field error metric is given by the Equivalent Error Signal, as specified by eq. (2).

$$EES_{E, E_{ref}}(\theta, \phi) = 20 \log_{10} \left(\frac{||E(\theta, \phi)| - |E_{ref}(\theta, \phi)||}{\max |E_{ref}(\theta, \phi)|} \right) \quad (2)$$

The result of this measurement, shown in Fig. 4 is not in good agreement with the complex reference pattern, indicating an improper convergence of the retrieved phase.

The reason for this result is the insufficient separation between spheres allowed by the setup, resulting in two sets of near-field measured magnitudes with very small relative difference (seen in Fig. 2). As a consequence, the two-scans technique converges to a local minimum of the space solution, or progresses very slowly towards the optimal solution, making phase retrieval unpractical. This observation is in line with previous experiences in both spherical and planar setups that showed better results of the two-scans technique with a larger difference between measured magnitudes [17][18]. Measurement noise, or high-order modes are ruled out as the reason for this result, because modal-filtered near-fields at the same radii, free from these errors, produce a similarly incorrect result.

B. Phase retrieval for measurement spheres with large separation

Despite the small movement of the probe positioner, different phaseless measurements of the VAST12 antenna can still be constructed using SWE to calculate new near-field signals on different spheres with greater separation, and thus larger variation of the magnitudes. The objectives of this is both to test the conclusions from the previous Subsection, and to study the possibility of achieving a more accurate phaseless measurement of the AUT. To this end, this Subsection presents an investigation of the accuracy of phase retrieval of the VAST12 as a function of sphere separation. In all cases one sphere is Measurement 1 at $r = 5853$ mm; and in order to ensure independence of the two sets of data, the calculated sphere is obtained through transformation of Measurement 2 to a different sphere. For this test a smaller number of 300

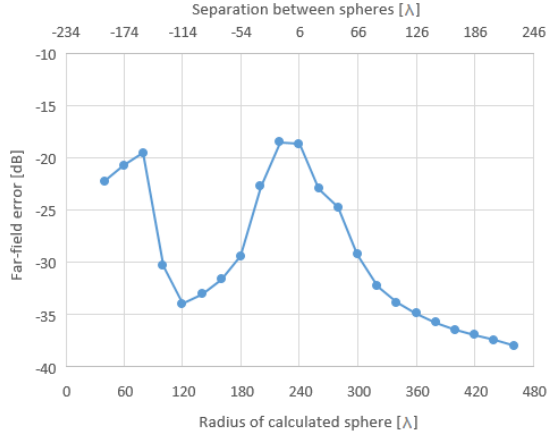


Fig. 5. Averaged far-field error over a range of $\theta < 50$ of phaseless measurements with different separation between measurement spheres.

iterations is used for each phase retrieval, due to the long processing time involved, of up to 24 hours for the previous 50,000 iterations of Section IV.A.

The error of the phaseless measurement E , compared to the complex reference field E_{ref} is calculated over a range of $\theta < 50$ deg as indicated by the following equation.

$$\epsilon_{\theta_0} = 20 \log_{10} \left(\frac{1}{N} \sum_{\theta_0} \frac{||E(\theta, \phi)| - |E_{ref}(\theta, \phi)||}{\max |E_{ref}(\theta, \phi)|} \right) \quad (3)$$

Where the θ_0 index of the summation denotes points of the far-field that are within an angular range of $\theta < \theta_0$ deg and N the total number of far-field points in this interval. Therefore, eq. (3) can be understood as an adaptation of eq. (2) when averaged in a certain interval of far-field directions.

Fig. 5 collects the result of comparing the complex reference with a series of phaseless measurements with different radii of the calculated sphere. The negative values of separation between spheres seen in the figure signify radius of the calculated sphere smaller than the measured sphere (thus, the field is backwards propagated), and a positive separation means that the calculated sphere is larger (forward propagation).

In Fig. 5 it is seen that as expected the far-field error of the phaseless measurement peaks when the two measurement spheres are at their closest, and becomes smaller as separation between spheres increases, both backwards or forwards. For smaller calculated spheres, a clear valley is seen in the interval of 100 to 200 wavelengths radius of the calculated sphere, but error becomes larger again for smaller radii, therefore when the calculated sphere is too close to the minimum sphere enclosing the AUT. For this AUT the smallest measurement radius that avoids intersection of the AUT and probe minimum spheres is about 0.8 m (32λ). The smallest tested radius is 40λ .

From Fig. 5 it is clear that the range of possible separation between measurement spheres is bounded by the physical dimensions of the measurement facility (upper limit) as well as the dimensions of the minimum sphere of the AUT and probe (lower limit).

In light of this, a proper phase retrieval is attempted using again a larger number 50,000 iterations, akin to Subsection

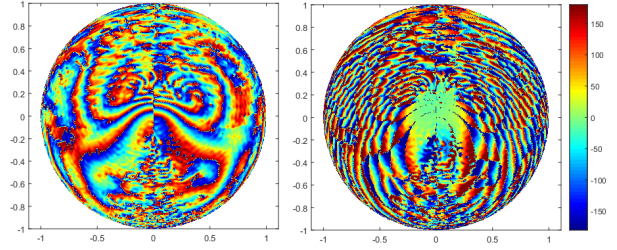


Fig. 6. Forward hemisphere phase u-v plots of retrieved near-field ϕ component at nominal distance of 5.8 m (left) and difference in phase with measured phase from Fig. 3 (right).

IV.A. From the results in Fig. 5 it is seen that a calculated near-field magnitude at a smaller radius of 3 m (120λ) in combination with a measured magnitude at a larger radius of 5.8 m (234λ) provided the smallest far-field error in the previous experiment (using a smaller calculated sphere). This combination is therefore used for the complete phase retrieval. It is seen in Fig. 2 that the magnitude in this sphere differs significantly from that of Measurement 1, and that both are significantly different from the far-field (see Fig. 7 below). This measurement represents a "realistic" scenario that could be potentially replicated within the dimensions of the DTU-ESA Facility, provided that the sufficient separation between measurement spheres of 2.8 m was allowed by the probe positioner.

In Fig. 6 the retrieved near-field phase of the ϕ component over the forward hemisphere is shown. This phase is compared with the measured ϕ phase in Fig. 3. It can be seen in Fig. 6 that the difference between retrieved and measured phases is close to zero in the central region of the forward hemisphere, where the magnitude of the signal is stronger, and then drifts from the measured phase outside of this central region as the magnitude level becomes much smaller.

The far-field pattern in Fig. 7 clearly shows a significant improvement of the phase retrieval compared to the previous case in Subsection IV.A, with a retrieved pattern which is in clear agreement with the complex reference within the main beam region, and with less than -35 dB on-axis error. Below -35 dB the phaseless measurement still provides a qualitative agreement with the side-lobe level and structure of the reference pattern. The cross-polar component is also retrieved with remarkable accuracy in the $\phi = 0$ plane. In addition to this, the radiation over the entire forward hemisphere is shown in Fig. 8; the u-v plot of the EES from Eq. (2) shows that the error of the phaseless measurement is below -35 dB over the entire forward hemisphere.

Finally, a third "unrealistic" phaseless measurement is tested using a new calculated magnitude at a radius of 25 m; this sphere is well within the near-field region of the AUT, which has a Rayleigh distance of 42 m, but is significantly larger than the dimensions of the DTU-ESA Facility. Again a Hertzian dipole is used as initial guess and the number of iterations is set 50,000. The resulting phaseless measurement in Fig. 9 show that, as the separation between spheres further increases to 19 m, accuracy of the phaseless measurement becomes even better than in the previous measurement.

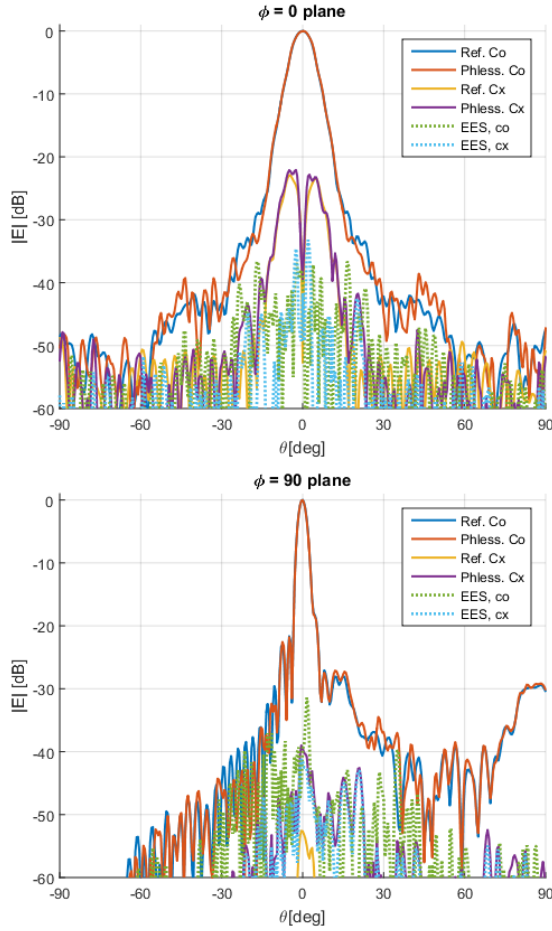


Fig. 7. E-plane ($\phi = 90$) radiation pattern of phaseless measurement using a smaller calculated sphere of $r = 3$ m, compared to reference complex measured pattern by means of EES.

V. SPHERICAL VS PLANAR PHASELESS MEASUREMENTS

During the course of the project from which this work stems (see Section VII) significant experience has been gained on the performance of phase retrieval with the two-scans technique in both planar and spherical setups. A main conclusion that is derived from this experience is the superior performance of spherical phaseless measurements compared to planar. The main advantage of spherical phase retrieval lay in its greater robustness to choice of initial guess compared to planar measurements. Planar phase retrieval is highly dependent of this choice: more accurate and complex initial guesses lead to better results [19]; this in turn implies planar phase retrieval requires more a priori knowledge of the AUT and its near-field. On the other hand, accurate spherical phase retrieval has been demonstrated with a simple Hertzian dipole phase guess [10]. Additional advantages are the accurate phase retrieval even with similar sampling as used in regular complex measurements, and concurrent retrieval of the two orthogonal components of the field, instead of being independently recovered as in the planar case.

The superior accuracy demonstrated by spherical phase retrieval, compared to planar phase retrieval, is due to the following principle factors:

- Unlike planar measurements, in which the near-field is sampled over a truncated plane in space, spherical acquisition is done over a sphere completely encompassing the AUT, thus it is entirely free of error due to near-field truncation.
- Measurement distance in planar measurements is much smaller than in spherical due to truncation, therefore spherical measurements can allow for much larger separation between measurement surfaces than typically used in planar phase retrieval [17],[19].
- Due to the larger measurement distances involved in spherical data acquisition, phase retrieval in a spherical setup is less affected by multiple reflections between AUT and probe.
- In spherical measurements the probe is pointing at the origin of coordinates of the AUT, unlike in planar measurements where the probe is scanned in front of the AUT (or viceversa); therefore spherical phaseless measurements are less sensitive to probe correction than planar phaseless measurements.

VI. CONCLUSIONS

A case of spherical phaseless measurements of the 12GHz VAST antenna has been presented and discussed, using purely measured data as well signals calculated from measurements by means of spherical wave expansion.

Spherical phaseless measurements were tested in an experimental case with two independent sets of measured magnitude at different radii, in contrast with previous experimental results which relied in near-field data obtained by means of backprojection of the measured far-field signal. The result of these measurements was negative as convergence of the phase was insufficient due to the small separation between measurement spheres allowed by the setup, and the small level of relative difference between the measured probe signals. It was thus concluded that for the current setup and AUT a phaseless measurement was not suitable.

Despite this, the use of additional signals obtained by means of spherical wave expansion at larger separations between measurement spheres than physically allowed by the probe positioner yielded much better results. A study of accuracy of phase retrieval for different separation between spheres shows that phase retrieval performs better with larger separation between measurements, provided that the measurement spheres are far enough from the minimum sphere of the AUT.

It has been demonstrated that a relatively complex radiation pattern such as the VAST12 can be recovered with significant accuracy of less than -35 dB error using a calculated near-field in a sphere of 3 m radius in addition to a measured sphere of 5.8 m radius. This measurement scenario can be plausibly performed within the dimensions of the DTU-ESA Facility, provided that this range of probe displacement was allowed by its positioner; it is therefore of great future interest. It has also been shown that even more accurate phase retrieval is possible by further increasing the separation between measurements, although the sphere used in this case is larger than physically allowed by the measurement facility.

Finally, it has been concluded that spherical phase retrieval offers superior results to planar phase retrieval; this is intu-

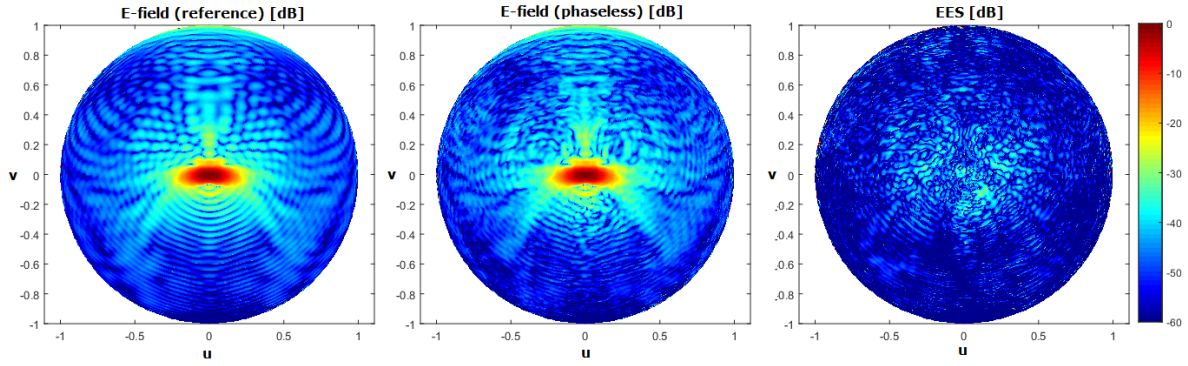


Fig. 8. u-v plots over the forward hemisphere of complex reference co-polar pattern of VAST12 (left) showing its characteristic elliptical main beam, of the retrieved phaseless co-polar pattern using a calculated sphere at $r = 3$ m (center), and Equivalent Error Signal (EES) between reference and phaseless patterns over the forward hemisphere (right).

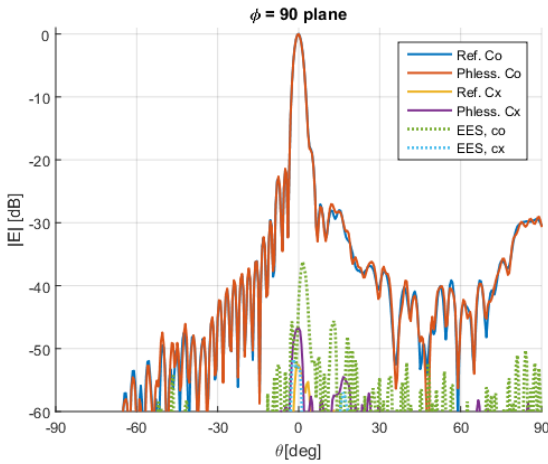


Fig. 9. E-plane ($\phi = 90$) radiation pattern of phaseless measurement using a larger calculated sphere of $r = 25$ m. compared to reference complex measured pattern by means of EES.

itive given that spherical complex near-field measurements are inherently superior to complex planar measurements.

VII. ACKNOWLEDGEMENT

This work was supported by the European Space Agency through ESA contract no. 4000113496/15/NL/Mh/ats "Phaseless Near Field Antenna Measurements". The authors thank ESA and ESA Technical Officer Maurice Paquay for the cooperation.

REFERENCES

- [1] A. P. Anderson, and S. Sali, "New possibilities for phaseless microwave diagnostics", *IEEE Proceedings H (Microwaves, Antennas and Propagation)*, vol. 132, no. 5, pp.291-298, 1985.
- [2] T. Isernia, G. Leone, and R. Pierri, "Phaseless Near Field Techniques: Formulation of the Problem and Field Properties", *Journal of Electromagnetic Waves and Applications*, vol. 8, no. 7, pp. 871-888, 1994 and "Phaseless Near Field Techniques: Uniqueness Conditions and Attainment of the Solution", *Journal of Electromagnetic Waves and Applications*, vol. 8, no. 7, pp. 889-908, 1994.
- [3] S.F. Razavi and Y. Rahmat-Samii, "A New Look at Phaseless Planar Near-Field Measurements: Limitations, Simulations, Measurements, and a Hybrid Solution", *IEEE Antennas and Propagation Magazine*, vol. 49, no. 2, pp. 170-178, April 2007.
- [4] T. Isernia, G. Leone, and R. Pierri, "Radiation Pattern Evaluation from Near-Field Intensities on Planes", *IEEE Transactions on Antennas and Propagation*, vol. 44, no. 5, pp. 701-710, 1996.
- [5] R.G. Yaccarino and Y. Rahmat-Samii, "Phaseless bi-polar planar near-field measurements and diagnostics of array antennas", *IEEE Transactions on Antennas and Propagation*, vol. 47, no. 3, pp. 574-583, March 1999.
- [6] S.F. Razavi and Y. Rahmat-Samii, "Polarization Extraction in Planar Near-Field Phaseless Measurements", *IEEE Transactions on Antennas and Propagation*, vol. 56, no. 10, pp 3233-3240, October 2008.
- [7] O. Breinbjerg and J. Fernandez Alvarez, "Phaseless Near-Field Antenna Measurement Techniques — An Overview", *Proceedings of the 38th Annual Symposium of the Antenna Measurement Techniques Association*, Austin, TX, USA, pp 314–319, 2016.
- [8] C.H. Schmidt, S.F. Razavi, T.F. Eibert, and Y. Rahmat-Samii, "Phaseless Spherical Near-Field Antenna Measurements for Low and Medium Gain Antennas", *Advances in Radio Science*, vol. 8, pp. 43-48, 2010.
- [9] G. Schnattinger, C. Lopez, E. Kihc, and T.F. Eibert, "Fast Near-Field Far-Field Transformation for Phaseless and Irregular Antenna Measurement Data", *Advances in Radio Science*, vol. 12, pp. 1-7, 2014.
- [10] M.F. Palvig, O. Breinbjerg, and S. Pivnenko, "Comparison of Two Phase Retrieval Methods for Phaseless Spherical Near-Field Antenna Measurements", *unpublished*, 2016.
- [11] O. Breinbjerg, S. Pivnenko, O.S. Kim, and J.M. Nielsen. "Recent Advances in Antenna Measurement Techniques at the DTU-ESA Spherical Near-Field Antenna Test Facility". *Proceedings of the 31st Ursi General Assembly and Scientific Symposium (Ursi Grass)*. IEEE, 6929026. 2014.
- [12] J.M. Nielsen, S. Pivnenko, and O. Breinbjerg, "Advanced Spherical Near-Field Antenna Measurement Techniques". *Proceedings of the 5th European Conference of Antennas and Propagation*. IEEE. 2011.
- [13] J. Lemarczyk, O.Breinbjerg, J.E. Hansen and J. Heeboll, "Definition and Design of a Standard Antenna for Antenna Test Range Validation". *Seventh International Conference on Antennas and Propagation ICAP 91*. 333. Inst Electrical Engineers: 926-29. 1991.
- [14] O. Breinbjerg, S. Pivnenko, M. Castaner, C. Sabatier, "Antenna Measurement Facility Comparison Campaign within the European Antenna Centre of Excellence". *Antennas and Propagation Society International Symposium*. IEEE 4. IEEE: 85:88. 2005.
- [15] S. Pivnenko, et al. "Comparison of Antenna Measurement Facilities with the DTU-ESA 12 GHz Validation Standard Antenna within the EU Antenna Centre of Excellence". *IEEE Transactions on Antennas and Propagation*, vol. 57, no. 7, pp 1863–1878, 2009.
- [16] J.E. Hansen (Ed.), "Spherical Near-Field Antenna Measurements", Peter Peregrinus Ltd. , London 1988.
- [17] J. Fernandez Alvarez, S. Pivnenko, and O. Breinbjerg. "Probe-Corrected Phaseless Planar Near-Field Antenna Measurements at 60 GHz", *Proceedings of the 37th Annual Symposium of the Antenna Measurement Techniques Association*, Long Beach, CA, USA, pp 314–319, 2015.
- [18] J. Fernandez Alvarez, and O. Breinbjerg, "Towards Planar Phaseless Near-Field Measurements of ESA's JUICE Mission 600 GHz SWI Reflector Antenna", *Proceedings of the 38th Annual Symposium of the Antenna Measurement Techniques Association*, Austin, TX, USA, 2016.
- [19] J. Fernandez Alvarez, and O. Breinbjerg, "A Computational and Experimental Investigation of $\lambda/2$ and $\lambda/4$ Sampling Step in Phaseless Planar Near-Field Measurements at 60GHz", *Proceedings of the 12th European Conference of Antennas and Propagation*. IEEE., London, UK, 2018.